MITSUBISHI HEAVY INDUSTRIES, LTD.
16-5, KONAN 2-CHOME, MINATO-KU
TOKYO, JAPAN

September 17, 2008

Document Control Desk
U.S. Nuclear Regulatory Commission
Washington, DC 20555-0001

Attention: Mr. Jeffrey A. Ciocco,

Docket No. 52-021
MHI Ref: UAP-HF-08174

Subject: MHI's Responses to NRC's Requests for Additional Information on Advanced Accumulator for US-APWR Topical Report MUAP-07001-P, Revision 1

With this letter, Mitsubishi Heavy Industries, LTD. ("MHI") transmits to the U.S. Nuclear Regulatory Commission ("NRC") the document entitled "MHI's Responses to NRC's Requests for Additional Information on Advanced Accumulator for US-APWR Topical Report MUAP-07001-P, Revision 1" a document package that responds to the NRC's Requests for Additional Information dated August 19, 2008.

As indicated in the enclosed materials, this document contains information that MHI considers proprietary, and therefore should be withheld from public disclosure pursuant to 10 C.F.R. § 2.390 (a)(4) as trade secrets and commercial or financial information which is privileged or confidential. A non-proprietary version of the document is also being submitted with the information identified as proprietary redacted and replaced by the designation "[   ]".

This letter includes a copy of the proprietary version (Enclosure 2), a copy of the non-proprietary version (Enclosure 3), and the Affidavit of Yoshiki Ogata (Enclosure 1) which identifies the reasons MHI respectfully requests that all materials designated as "Proprietary" in Enclosure 2 be withheld from public disclosure pursuant to 10 C.F.R. § 2.390 (a)(4).

Please contact Dr. C. Keith Paulson, Senior Technical Manager, Mitsubishi Nuclear Energy Systems, Inc. if the NRC has questions concerning any aspect of the submittal.   His contact information is below.

Sincerely,

Yoshiki Ogata,
General Manager- APWR Promoting Department
Mitsubishi Heavy Industries, LTD.

Enclosures:
1 - Affidavit of Yoshiki Ogata

2 - MHI's Responses to NRC's Requests for Additional Information on Advanced Accumulator for US-APWR Topical Report MUAP-07001-P, Revision 1 (proprietary)

3 - MHI's Responses to NRC's Requests for Additional Information on Advanced Accumulator for US-APWR Topical Report MUAP-07001-P, Revision 1 (non-proprietary)

CC: J. A. Ciocco
    C. K. Paulson

Contact Information
    C. Keith Paulson, Senior Technical Manager
    Mitsubishi Nuclear Energy Systems, Inc.
    300 Oxford Drive, Suite 301
    Monroeville, PA 15146
    E-mail: ckpaulson@mnes-us.com
    Telephone: (412) 373-6466

MITSUBISHI HEAVY INDUSTRIES, LTD.

AFFIDAVIT

I, Yoshiki Ogata, state as follows:

1. I am General Manager, APWR Promoting Department, of Mitsubishi Heavy Industries, LTD ("MHI"), and have been delegated the function of reviewing MHI's US-APWR documentation to determine whether it contains information that should be withheld from public disclosure pursuant to 10 C.F.R. § 2.390 (a)(4) as trade secrets and commercial or financial information which is privileged or confidential.

2. In accordance with my responsibilities, I have reviewed the enclosed document entitled "MHI's Responses to NRC's Requests for Additional Information on Advanced Accumulator for US-APWR Topical Report MUAP-07001-P, Revision 1" dated September 2008, and have determined that portions of the document contain proprietary information that should be withheld from public disclosure. Those pages containing proprietary information are identified with the label "Proprietary" on the top of the page and the proprietary information has been bracketed with an open and closed bracket as shown here "[   ]". The first page of the document indicates that all information identified as "Proprietary" should be withheld from public disclosure pursuant to 10 C.F.R. § 2.390 (a)(4).

3. The information identified as proprietary in the enclosed document has in the past been, and will continue to be, held in confidence by MHI and its disclosure outside the company is limited to regulatory bodies, customers and potential customers, and their agents, suppliers, and licensees, and others with a legitimate need for the information, and is always subject to suitable measures to protect it from unauthorized use or disclosure.

4. The basis for holding the referenced information confidential is that it describes the unique design of the Advanced Accumulator developed by MHI and not used in the exact form by any of MHI's competitors. This information was developed at significant cost to MHI, since it required the performance of Research and Development and detailed design for its software and hardware extending over several years.

5. The referenced information is being furnished to the Nuclear Regulatory Commission ("NRC") in confidence and solely for the purpose of information to the NRC staff.

6. The referenced information is not available in public sources and could not be gathered readily from other publicly available information. Other than through the provisions in paragraph 3 above, MHI knows of no way the information could be lawfully acquired by organizations or individuals outside of MHI.

7. Public disclosure of the referenced information would assist competitors of MH in their design of new nuclear power plants without incurring the costs or risks associated with the design and testing of the subject systems. Therefore, disclosure of the information contained in the referenced document would have the following negative impacts on the competitive position of MH in the U.S. nuclear plant market:

A. Loss of competitive advantage due to the costs associated with development and testing of the Advanced Accumulator. Providing public access to such information permits competitors to duplicate or mimic the Advanced Accumulator design without incurring the associated costs.

B. Loss of competitive advantage of the US-APWR created by benefits of enhanced plant safety, and reduced operation and maintenance costs associated with the Advanced Accumulator .

I declare under penalty of perjury that the foregoing affidavit and the matters stated therein are true and correct to the best of my knowledge, information and belief.

Executed on this 17th day of September, 2008.

Yoshiki Ogata,
General Manager- APWR Promoting Department
Mitsubishi Heavy Industries, LTD.

Enclosure 3

UAP-HF-08174
Docket No. 52-021

**MHI's Responses to NRC's Requests
for Additional Information**

on

**Advanced Accumulator for US-APWAR Topical Report MUAP-
07001-P, Revision 1**

September 2008

RAI 1.

During early large flow injection period, the angular momentum of the flows from the standpipe and the small pipe cancel in the vortex chamber (See response to NRC question 2, and Eq. 2.1). These flows will decrease as the accumulator depressurizes and the level decreases. Does this angular momentum cancellation happen for all flows? Can there be some vortex during this time period?

Response

The angular momentum cancellation happens for all flow during large flow injection under the plant operating conditions for which friction loss is negligible across both the small flow pipe and the standpipe to the large flow pipe. This can be seen as follows,

Let flow loss coefficient of the small flow pipe be ζ_2, and that of the standpipe to the large flow pipe ζ_1. Both ζ_2 and ζ_1 are composed of form resistances because friction on them is negligible. The pressure drop across the standpipe to the large flow pipe, ΔP, is identical to that across the small flow pipe, and is given by:

$$\Delta P = \zeta_1 \frac{1}{2} \rho V_1^2 = \zeta_2 \frac{1}{2} \rho V_2^2 \tag{1-1}$$

The notations are the same as those in the response to Question-2 in the first set of NRC RAIs on the Advanced Accumulator.

Equation (1.1) can be expressed as

$$\frac{Q_1 V_1}{Q_2 V_2} = \frac{A_1}{A_2} \frac{\zeta_2}{\zeta_1} = consant, \tag{1-2}$$

where A_1 and A_2 are cross sectional areas of the large and small flow pipes respectively.

Equation (2.1) in the response to Question-2 rewritten below, hence, holds for all flow of the flow damper.

$$\left[\qquad\qquad\qquad\qquad\qquad\qquad\qquad \right] \tag{2.1}$$

There is, consequently, no vortex during the large flow injection because there is no angular momentum that is expressed by Equation (2.1).

RAI 2.

Cavitation will occur at the lowest pressure location. In the preliminary computational fluid dynamic (CFD) analysis (see Fig. 1) that NRC performed, cavitation occurred during large flow rate conditions just downstream the throat of the nozzle.

a. Can you quantify this cavitation occurrence?

b. Can there be cavitation at the center of vortex where pressure will be low? Is the cavitation in the vortex center scale-dependent?

Response

a..

Yes.
As mentioned in the book "Cavitation" by R. T. Knapp et al., McGraw-Hill 1970, the inception of cavitation and its magnitude can be quantified with a cavitation parameter (or a cavitation factor). MHI uses a cavitation factor as one of the main parameters of the flow rate coefficients for the flow damper.

b.
The response that follows assumes that cavitation of interest occurs at the center of a vortex during small flow rate conditions. Under small flow rate conditions, there can be a stable cavitation cloud at the center of a vortex.
The size of cavitaion cloud will be scale-dependent, but it does not affect the flow-rate coefficients, as shown below.
The cavitation cloud does not restrict the flow area because of the effect of the reducer between the outlet port and the throat of the nozzle. The cavitation cloud will be formed at the center of the outlet of the vortex chamber, and water will flow on its periphery. Then, the reducer will guide the water flow to the throat so that the cavitation cloud is contained within the space of the reducer, resulting in constant flow-rate coefficients.

RAI 3.

Will there be any choked flow at the throat of the outlet pipe?

Response

There will not be any choked flow at the throat of the outlet pipe under the plant operating conditions.
During large flow injection, cavitation may occur on the periphery of the diffuser downstream the throat, and result in reduced flow-rate coefficients. Since the pressure downstream of the throat under choked flow is reduced to vapor pressure, the flow rate becomes a function of only the tank pressure and is independent of the pressure at the exit of the injection pipe. Test data shows that all the flow rate collapses onto a single curve during large flow injection, so we believe there is no choked flow under these test conditions under plat operating conditions.

During small flow injection, cavitation may occur at the center of a vortex and be contained in the space of the reducer, as discussed in the answer to RAI 2-b. Hence, there is no choked flow during small flow injection. This is supported by experimental data showing constant flow-rate coefficients, during small flow injection.

RAI 4.

The dissolved gas will come out of the coolant as the pressure decreases. How does that affect the pressure drop?

Response

According to the observation of bubbles in a full-height 1/2-diameter accumulator tank under actual operating pressures and nitrogen saturation, tiny bubbles with diameters of about 0.04 to 0.08 inches (1 to 2 mm) appear at the start of flow injection and ascend to the free surface of the water due to their buoyancy. If some of these tiny bubbles are entrained in the flow into the vortex damper, they can reduce the apparent density of water, and causes a reduction in the flow rate coefficients for the flow damper. However, since the diffusion coefficient of nitrogen is very small as discussed below in the answer to RAI 5-b, bubbles cannot increase significantly in the very short time (less than 1 sec) during which the bubbles go through the flow damper.

RAI 5.

According to the topical report, there is no Nitrogen coming out of the tank.

a. How was this measured?

b. What will be the nitrogen solubility in the actual accumulator? Will it be in
equilibrium? Do all the tests have equilibrium nitrogen solubility? How much
nitrogen will come out of the solution in the vortex chamber and at the throat?

Response

a.
MHI measured the water level in the standpipe with an electrode water-level meter that
consists of many electrodes spaced along the wall of the standpipe. The test data showed
that the water level stayed in the standpipe under all test conditions.

The water level in the standpipe was measured using twenty-two electrodes located along the
vertical line on the wall of the standpipe, as shown in Figure 28-3 "Stand Pipe (Full height 1/2
scale model)" outline drawing (refer to No.11 Water Level Gauge Connection). Every
electrode generates a signal output under water, which stops in the gas space. Therefore, the
circular marks on the curves of the transient of the water level in the standpipe (Figure 4.2.4-5
- 4.2.4-11 in the topical report) indicate that the electrodes attached at the corresponding
levels are immersed in water.

b.
Nitrogen solubility
The calculated dissolved nitrogen by molecular diffusion in liquid in the actual accumulator is
as follows:

Time	Dissolved Ratio (to saturated-dissolved nitrogen)
2 years	12 %
5 years	17 %
10 years	24%

According to the calculation's result, nitrogen will not be saturated in the actual accumulator by
molecular diffusion only.

Equilibrium nitrogen solubility
Nitrogen gas was forced to be dissolved in the liquid in case 5 only (Refer to Table 4.2.4-1 and
Fig. 4.2.4-9 in the topical report). In other cases, nitrogen gas was passively-charged so that it
was not in equilibrium.

How much nitrogen will come out of the solution
A sharp drop of pressure occurs in the vortex chamber and at the throat. For a flow rate of
5000 gpm in the 1/2 scale model, the total traveling time of fluid across the vortex chamber
and the throat is about 0.15sec. The diffusion coefficient of nitrogen is about $3\times10^{-9}m^2/s$ in
water at 300°K, while its kinematic viscosity is $0.857 \times10^{-6}m^2/s$. These figures indicate that the
diffusion speed of nitrogen is about 1/1000 of its momentum in water. Since the effect of
friction is negligibly small in the flow damper which is controlled by viscosity, the diffusion of
nitrogen is also negligibly small during the short duration of 0.15 sec for which the flow passes

through. In other words, the amount of nitrogen coming out of solution in the vortex chamber and the throat is negligible.

RAI 6.

Section 3.3 of the topical report mentions Zobel Diode and the response to NRC Question 5 also refers to a web site. This reference does not provide any quantitative information. Is there any other reference that guides the design of vortex flow damper?

Response

The article on the configurations and dimensions of the Zobel Diode, "Report of Subcommittee of Power Fluidics -Elements of Power Fluidics and their Application-," P-SC40 Report No.328, page 106, is written in Japanese and was published by Japanese Society of Mechanical Engineers, March 15, 1984. The chairperson of the subcommittee was Dr. Tatsuya Hagiwara. The original paper on the Zobel diode was "R. Zobel, Mitt. Hydraul. Inst. Munich, 8-19(1936)," which is perhaps unavailable today. MHI does not have the original paper.

RAI 7.

Table 3.3-1 of the topical report mentions the rationale for the shape and size of stand pipe, and the injection pipe throat area. Please provide quantitative arguments or references for the statements made in this table.

Response

Each standpipe dimension is determined as follows:
1) The standpipe height (1):
A) The configuration and the dimensions of the accumulator tank are decided based on the available space at the location where the tank will be set, the volumes of water involved in large and small flow injections, and the amounts of nitrogen gas and dead water.
B) The vortex chamber is placed at the bottom of the accumulator tank in order to minimize the volume of dead water which occupies the space beneath the small flow pipe.
C) The lower end of the skirt around the anti-vortex cap on the upper inlet of the standpipe is placed on the boundary between water volumes of large and small flow injections.
D) The standpipe is set between them and the height of the stand pipe is thus determined.
2) The length of the cross sectional area of the standpipe, denoted as Height of Standpipe inner section (2) at Table 3.3-1, is set equal to the width of the large flow pipe.
3) The width of the cross sectional area of the standpipe, denoted as Width of Standpipe inner section (3) at Table 3.3-1, is determined so that the cross sectional area of the standpipe is large enough to prevent nitrogen gas leakage passing through the standpipe. See the answer to RAI 18 below for the calculation method for the cross sectional area.
4) The inner diameter of the throat (4) is set so that the large flow rate can be accommodated from the design demand based on the characteristics of the flow damper, measured using a selected scale model.
For example, let's consider how the dimension of the flow damper is established for a flow rate, Q, under pressure difference, Δp, over the flow damper and the injection pipe at an arbitrary moment during the large flow injection based on the flow-rate coefficient, C_v of a selected model. Let the flow resistance coefficient of the injection pipe be ζ_p which is given by the design condition. The pressure balance is given by:

$$\Delta p = \left(\frac{1}{C_v^2} + \zeta_p\right)\frac{1}{2}\rho\left(\frac{Q}{A}\right)^2 \tag{7-1}$$

where A is the cross sectional area of the referenced injection pipe. The arbitrary moment during the large flow injection can be chosen as the initial moment, a middle moment or the last moment just before switching the flow from large to small flow injection. Equation (7-1) is written as:

$$A = Q\sqrt{\left(\frac{1}{C_v^2} + \zeta_p\right)\frac{\rho}{2\Delta p}} \tag{7-2}$$

The diameter of the referenced injection pipe, D_p is

$$D_p = \sqrt{\frac{4A}{\pi}} \tag{7-3}$$

The ratio of the diameter of the throat to that of the referenced injection pipe for the model selected to US-APWR is

$$\left[\qquad\qquad \right] \tag{7-4}$$

The diameter of the throat is, thus, given as

$$\left[\qquad\qquad\qquad \right]$$ (7-5)

5) The ratio of the diameter of the throat of the actual flow damper, d_t, to that of the selected scale model is applied to all the dimensions of the standpipe, flow damper and the outlet nozzle to maintain the similarity of the flow damper. It establishes all the other dimensions such as (5) Inner diameter and (6) Height of the vortex chamber, (7) and (8) Widths of small and large flow pipe, (9) Angle of collision, or Facing angle of large flow pipe and small flow pipe, and (10) Diffuser angle, or Expansion angle of the throat. If the cross sectional area of the standpipe is not compatible with that given in Item 3) above, the width determined from Item 3) shall be adopted. The performance of the flow damper is demonstrated by the experimental data and how to select each dimension of the flow damper is based on the phenomena predicted and MHI's know-how.

RAI 8.

Figure 4.3-1 of the topical report shows the results for the 1/2 and 1/5 scale facilities. For the low flow injection case the flow rate coefficient seems to be almost independent of the cavitation factor. Does this mean that there is no gas phase in the flow path?

Response

See the answer to RAI 2-b.

RAI 9.

Section 4.3 of the topical report has alluded to Froude number and Reynolds number.

a. Please show analytically (through balance equations) the relevant non-dimensional groups with justification for the reference quantities.

b. Provide a dimensional analysis using Pi groups to demonstrate that C_v is a function of σ_v only in this process. As the water level changes so do the velocity values thus,

· Reynolds Number or any dimensionless number involving velocity and probably shear stress should be part of the analysis.

c. Using preliminary CFD analysis, Nitrogen was observed at the exit of the injection pipe. If this is the case, the presence of Nitrogen should be accounted for in the dimensionless analysis.

Response

a.
Since the flow in the advanced accumulator is an initial- and boundary-value problem, the similarity law has to be satisfied for the following three items:
1) Governing Equations: (1) equation of continuity and (2) equation of motion,
2) Boundary Conditions: (3) boundary configurations, (4) inlet condition, and (5) outlet condition, and
3) Initial Conditions: (6) Initial flow in the accumulator tank including the standpipe, the flow damper and the outlet nozzle and (7) Initial flow in the injection pipe.

The equations of energy and state are not necessary for incompressible flow. The dimensionless forms of (1) equation of continuity and (2) equation of motion, or Navier-Stokes equation, are as follows:

$$\left(\nabla^* \cdot \mathbf{u}^*\right) = 0, \tag{9-1}$$

$$\frac{\partial u^*}{\partial t^*} + \left(u^* \cdot \nabla^*\right)u^* = -\nabla^*\left(\frac{p}{\rho U^2}\right) + \frac{1}{Re}\Delta^* u^*, \tag{9-2}$$

where u is a velocity vector, t time, p pressure, ρ density of fluid, and ν kinematic viscosity of fluid. Nabla, ∇, and delta, Δ, are defined as:

$$\nabla = \left(\frac{\partial}{\partial x}, \frac{\partial}{\partial y}, \frac{\partial}{\partial z}\right), \quad \text{and} \quad \Delta = \nabla^2 = \frac{\partial^2}{\partial x^2} + \frac{\partial^2}{\partial y^2} + \frac{\partial^2}{\partial z^2}.$$

Using a characteristic length, D, and a characteristic velocity, U, the asterisk * indicates dimensionless quantities as:

$$u^* \equiv \frac{u}{U}, \quad t^* \equiv \frac{t}{D/U}, \quad \nabla^* \equiv D\nabla, \quad \Delta^* \equiv D^2\Delta \quad \text{and} \quad Re \equiv \frac{DU}{\nu}.$$

The similarity of equation of continuity (9-1) is unconditionally satisfied. The similarity of equation of motion (9-2) is satisfied, if the Reynolds number, Re, is the same as that of the actual accumulator, or if the effect of Reynolds number is negligible. The Reynolds numbers for the models used for the development of the advanced accumulator are so large that the viscosity of the fluid does not affect the flow resistances of the flow damper and the injection pipe. Consequently, the similarity of the governing equations is satisfied.

The boundary configurations (3) of the full-height 1/2 scaled model are similar to those of the actual accumulator, excepting the heights of the test tank and the standpipe. The descending velocities of free surfaces both in the test tank and the standpipe are the same as those of the actual accumulator, and the transients of the inner boundaries, namely the water surfaces in the full-height test tank and the full-height standpipe, are similar to those of the actual accumulator. This is the reason why the deformed model, or the full-height 1/2-scaled model, was used for testing under actual pressure conditions. At the same time, the use of the actual descending velocities of the water surfaces assure the validity of the simulation of expansion of nitrogen gas in the test tank with respect to that in the actual accumulator tank. The similarity of the behavior of the water surfaces is satisfied with the Froude number identical to that of the actual accumulator. There is no inlet to the advanced accumulator, therefore the inlet condition (4) is inapplicable. The outlet condition (5) is the pressure at the exit of the injection pipe and was set as a test condition.
Consequently, the similarity of the boundary conditions is satisfied.
Initially, water in the system of the advanced accumulator tank (6) and the injection pipe (7) of the model is at rest as is the case in the full-scale accumulator, so the initial conditions are satisfied.

b.
I have a question to discuss the flow-rate coefficient with a dimensional analysis using the Pi theorem, because the flow in the flow damper and the injection pipe is a kind of internal flows that have been studied in detail by many researchers yet. The variation of water level and gas expansion affect the inlet pressure as a boundary condition of the flow damper, but not the flow resistance, which has a one-to-one correspondence with the flow-rate coefficient, C_v.
The flow-rate coefficient, C_v is defined as:

$$C_v = \frac{Q}{A\sqrt{2\,\Delta p/\rho}}$$ (9-3)

where Q is the flow rate, A the characteristic area, Δp the pressure difference across the system of the accumulator and the injection pipe, and ρ the density of fluid.
The pressure difference, $\Delta p = p_T - p_2$, is given by the gas pressures in the accumulator tank, p_T, and at the exit of the injection pipe, p_2. The gas pressure, p_T, is governed by the reduction of water level in the accumulator tank. The nitrogen gas changes adiabatically during large flow-rate injection, and polytropically during small flow-rate injection.
The gas volume at an arbitrary time t is;

$$V_G = V_{G0} + \int_0^t Q\,dt$$ (9-4)

The pressure in the accumulator tank, p_T, is given by the polytropic expansion expressed as;

$$p_T V_G{}^n = p_{T0} V_{G0}{}^n$$ (9-5)

where V_{G0} and P_{T0} are the initial values of nitrogen gas volume and pressure in the accumulator tank. The polytropic index n is set to 1.4 for the course of adiabatic expansion, while n can be some other value for general expansion of nitrogen.
Let D_T and H_T be the diameter and the height of the accumulator tank. The initial water level is given as:

$$h_0 = H_T - \frac{4V_{G0}}{\pi D_T{}^2}.$$ (9-6)

Mitsubishi Heavy Industries, LTD.

The velocity of the reduction in the water level in the accumulator tank, V_S, is:

$$V_S = \frac{4Q}{\pi D_T^2} \qquad (9\text{-}7)$$

Water level at time t is:

$$h = h_0 - \int_0^t V_s\, dt = H_T - \frac{4}{\pi D_T^2}\left(V_{G0} + \int_0^t Q\, dt\right) = H_T - \frac{4V_G}{\pi D_T^2}. \qquad (9\text{-}8)$$

Substituting Equations (9-7) and (9-8) into Equation (9-5) and modifying it yield:

$$p_T = p_{T0}\left(\frac{H_T - h_0}{H_T - h}\right)^n. \qquad (9\text{-}9)$$

The transient pressure in the accumulator tank is determined by this equation.
The pressure at the exit of the injection pipe, p_2, is given by the operating conditions of the plant, and can be excluded from the parameters discussed here.
If cavitation does not occur, the pressure difference between any local pressure, p, in the flow damper and the outlet pressure, p_2, is given by the product of a pressure coefficient, C_p, and dynamic pressure, $\rho U^2/2$ as;

$$p - p_2 = C_p \frac{1}{2}\rho U^2. \qquad (9\text{-}10)$$

As reflected in Equation (9-2), the dimensionless parameter of fluid property is only a Reynolds number that represent the effect of fluid viscosity. In other words, the pressure coefficient, C_p, is a function of a Reynolds number only for flow without cavitation.

If cavitation occurs, the minimum local pressure reduces and is kept to the critical pressure so that the pressure coefficient, C_p, at the local point where cavitaion occurs may vary. The critical pressure at which cavitation occurs will be close to the vapor pressure of the fluid for vaporous cavitaion, and higher than the vapor pressure for gaseous cavitaion. If we assume the local pressure, p, to be the vapor pressure, p_v, then Equation (9-10) yields

$$-C_p = -\frac{p_2 - p_v}{\rho U^2/2} \equiv K, \qquad (9\text{-}11)$$

which is an index of the cavitation state called the "cavitation factor" or "cavitation parameter".
The flow resistance coefficient is defined as:

$$\zeta \equiv \frac{\Delta p}{\rho U^2/2}, \qquad (9\text{-}12)$$

Thoma's sigma is defined as:

$$\sigma_v = \frac{p_2 - p_v}{\Delta p} = \frac{K}{\zeta}, \qquad (9\text{-}13)$$

It is also an index of the cavitation state.
If the pressure distribution changes not only due to viscous boundary layers, but also due to cavitation occurrence, the flow resistance coefficient, ζ, varies and becomes a function of the cavitation factor in addition to the Reynolds number. Using $U = Q/A$, substituting Equation (9-12) into Equation (9-3) yields:

$$C_v = \frac{1}{\sqrt{\xi}} \, .$$

(9-14)

Consequently, the flow rate coefficient is a function of the cavitation factor and the Reynolds number. If a form resistance is dominant and friction is negligible, the flow rate coefficient is independent of the Reynolds number and is a function only of the cavitation factor.

c.
As mentioned in the Answer to RAI 5-b, nitrogen will only diminish the superficial density of water in through the formation of tiny bubbles. Consequently, the above dimensionless analysis discussion is not affected by the release of nitrogen.

RAI 10.

Please show how non-dimensional groups are preserved in the different scaled facilities and the full scale accumulator. If there are any distortions, will they affect the flow and by how much? What will be the uncertainty in the flow rate coefficient and the cavitation parameter for the full scale application? Can the correlation developed between the flow rate coefficient and the cavitation parameters based on ½ scale test data predict the performance at lower scale (1/3.5 and 1/5) tests?

Response

The non-dimensional parameters are as follows:

Flow-rate Coefficient: $C_v = \dfrac{Q}{A\sqrt{2\Delta p/\rho}}$ (10-1)

Cavitaion Factor: $\sigma_v = \dfrac{p_2 - p_v}{\Delta p}$,   (10-2)

Reynolds Number: $Re = \dfrac{U D}{\nu}$,   (10-3)

Froude Number: $Fr = \dfrac{U}{\sqrt{g L}}$ (10-4)

The areas investigated with 1/5-, 1/3.5- and 1/2-scaled models were as follows:
1/5-scaled model: (1) development of components of the flow damper, (2) characteristics of flow-rates, (3) prevention of gas entrainment during flow switching.
1/3.5-scaled model: (1) examination of behavior of water surface before and during flow switching, and (2) effectiveness of the anti-vortex cap.
1/2-scaled model: (1) total characteristics of the advanced accumulator, including characteristics of flow-rates for both the large and small flow-rate periods, prevention of gas entrainment during flow switching, and (2) prediction of the characteristics of the full scale advanced accumulator.
MHI predicted the characteristics of the full scale advanced accumulator based on the 1/2-scaled model under the actual operating pressures. Using the suffices "m" and "p" for the parameters of the model and full-scale accumulators respectively, the comparisons of the parameters used in the 1/2-scaled model with respect to those of the full-scale accumulator are as follows:

Dimensions of flow damper and diameter of the tank: $D_m = \dfrac{D_p}{2}$

Area: $A_m = \dfrac{\pi}{4}D_m^2 = \dfrac{\pi}{4}\left(\dfrac{D_p}{2}\right)^2 = \dfrac{A_p}{4}$

Heights of the tank and the standpipe: $L_m = L_p$

Temperature of water: $T_m = T_p$ This gives density of fluid: $\rho_m = \rho_p$, kinematic viscosity: $\nu_m = \nu_p$, and vapor pressure: $p_{vm} = p_{vp}$.

Pressures and pressure difference: $p_{Tm} = p_{Tp}$, $p_{2m} = p_{2p}$ and $\Delta p_m = \Delta p_p$

Note1: The pressure at the exit of the injection pipe is given as constant for the 1/2-scaled model tests.
Velocity: $U_m = U_p$

Flow rate: $Qm = A_m U_m = \dfrac{A_p}{4}U_p = \dfrac{Qp}{4}$

Mitsubishi Heavy Industries, LTD.

Consequently, the non-dimensional parameters for the 1/2-scaled model have the relations with those of the full-scale accumulator as follows:

Flow-rate Coefficient: $C_{vm} = C_{vp}$ (10-5)

Cavitaion Factor: $\sigma_{vm} = \sigma_{vp}$,   (10-6)

Reynolds Number: $Re_m = \dfrac{Re_p}{2}$,   (10-7)

Froude Number: $Fr_m = Fr_p$ (10-8)

The influence of the distortion of Reynolds number was evaluated in Chapter 4.3 of the Topical Report and shown to be negligible.

Since the 1/5-scaled model tests were done under pressure conditions lower than those of the actual accumulator, test conditions were adjusted to make them suitable for the objective of each experiment.

The comparisons of quantities used in the 1/5-scaled model with respect to those of the full-scale accumulator are as follows:

Dimensions of flow damper and equivalent diameter of the tank: $D_m = \dfrac{D_p}{5}$

Area: $A_m = \dfrac{\pi}{4} D_m{}^2 = \dfrac{\pi}{4}\left(\dfrac{D_p}{5}\right)^2 = \dfrac{A_p}{25}$

Heights of the standpipe: $L_m = \dfrac{L_p}{5}$

Nitrogen gas volume in the tank: $V_{gm} = \dfrac{V_{gp}}{125}$

Temperature of water: $T_m = T_p$ This gives density of fluid: $\rho_m = \rho_p$, kinematic viscosity:

$\nu_m = \nu_p$, and vapor pressure: $p_{vm} = p_{vp}$.

To obtain the flow-rate characteristics of the flow damper, the nitrogen gas in the test tank was set at an arbitrary initial pressure under 1MPa, and the exit of the injection pipe was set at the atmospheric pressure. (Those levels do not represent those of the actual accumulator: their use, however, was acceptable to assess the flow rate characteristics of the flow damper, and to evaluate the effect of scaloffing on the flow damper performance.)

To confirm no gas entrainment at the flow switching, the Froude number of the 1/5-scaled model was set to be equal to that of the actual accumulator, and the flow in the vortex chamber was determined.

Froude Number: $Fr_m = \dfrac{U_m}{\sqrt{g\,L_m}} \equiv Fr_p = \dfrac{U_p}{\sqrt{g\,L_p}}$ (10-9)

The flow rate was given as: $Q_m = A_m U_m = \dfrac{A_p}{25} U_p \sqrt{\dfrac{L_m}{L_p}} = \dfrac{Q_p}{25\sqrt{5}}$.   (10-10)

The nitrogen gas pressure in the test tank was set as:

$$\Delta p_m = \dfrac{\rho}{2}\left(\dfrac{Q_m}{C_v A_m}\right)^2 = \dfrac{\rho}{2}\left(\dfrac{Q_p}{C_v A_p}\right)^2 \dfrac{L_m}{L_p} = \dfrac{L_m}{L_p}\Delta p_p .$$ (10-11)

The distortion of the flow-rate coefficient was assessed in Chapter 4.3 of the Topical Report, and the scale effect of the flow-rate characteristics was estimated. In other words, we can use

Flow-rate Coefficient: $C_{vm} = C_{vp}$ (10-12)

Cavitaion Factor: $\sigma_{vm} = \sigma_{vp}$, (10-13)

Reynolds Number: $Re_m = \dfrac{U_m D_m}{\nu} = \dfrac{U_p D_p}{5\sqrt{5}\,\nu} = \dfrac{Re_m}{5\sqrt{5}}$, (10-14)

The influence of the distortion of the Reynolds number for the 1/5-scale model was evaluated in Chapter 4.3 of the Topical Report and determined to be negligible, too.

The 1/3.5-scale model was part of the inlet of the standpipe and its vicinity. Since the behavior of the water surface in the test tank was being examined, the Froude number of the 1/3.5-scale model was set to be equal to that of the actual accumulator in Equation (10-9). Then, the flow rate was

$$Qm = A_m U_m = \dfrac{A_p}{3.5^2} U_p \sqrt{\dfrac{L_m}{L_p}} = \dfrac{Qp}{12.25\sqrt{3.5}} .$$ (10-15)

The flow rate was manually controlled and secured. By doing this, MHI assessed the behavior of the water level of the actual accumulator based on the similarity of the free surface of the actual accumulator and the scale model. There was no 1/3.5-scale model of the flow damper.

RAI 11.

Please provide one table summarizing all the similar dimensions for different facilities including the actual accumulator.

Response

Here is the comparison of the similar dimensions of the flow damper in each scale model and in the actual accumulator.

Table 11-1 Comparison of dimensions of flow damper in scale models and the actual ACC

| No.	region	Actual accumulator	Full Height 1/2 scale model	1/5 scale model
1	Standpipe Height (mm) (Height from the top of vortex chamber (mm))			
2	Height of standpipe Inner section (mm)			
3	Width of standpipe inner section (mm)			
4	Inner diameter of the throat			
5	Inner diameter of the vortex chamber (mm)			
6	Height of vortex chamber (mm)			
7	Width of small flow pipe (mm)			
8	Width of large flow pipe (mm)			
9	Facing angle of large and small flow pipe (°)			
10	Expansion angle of the throat (°)			
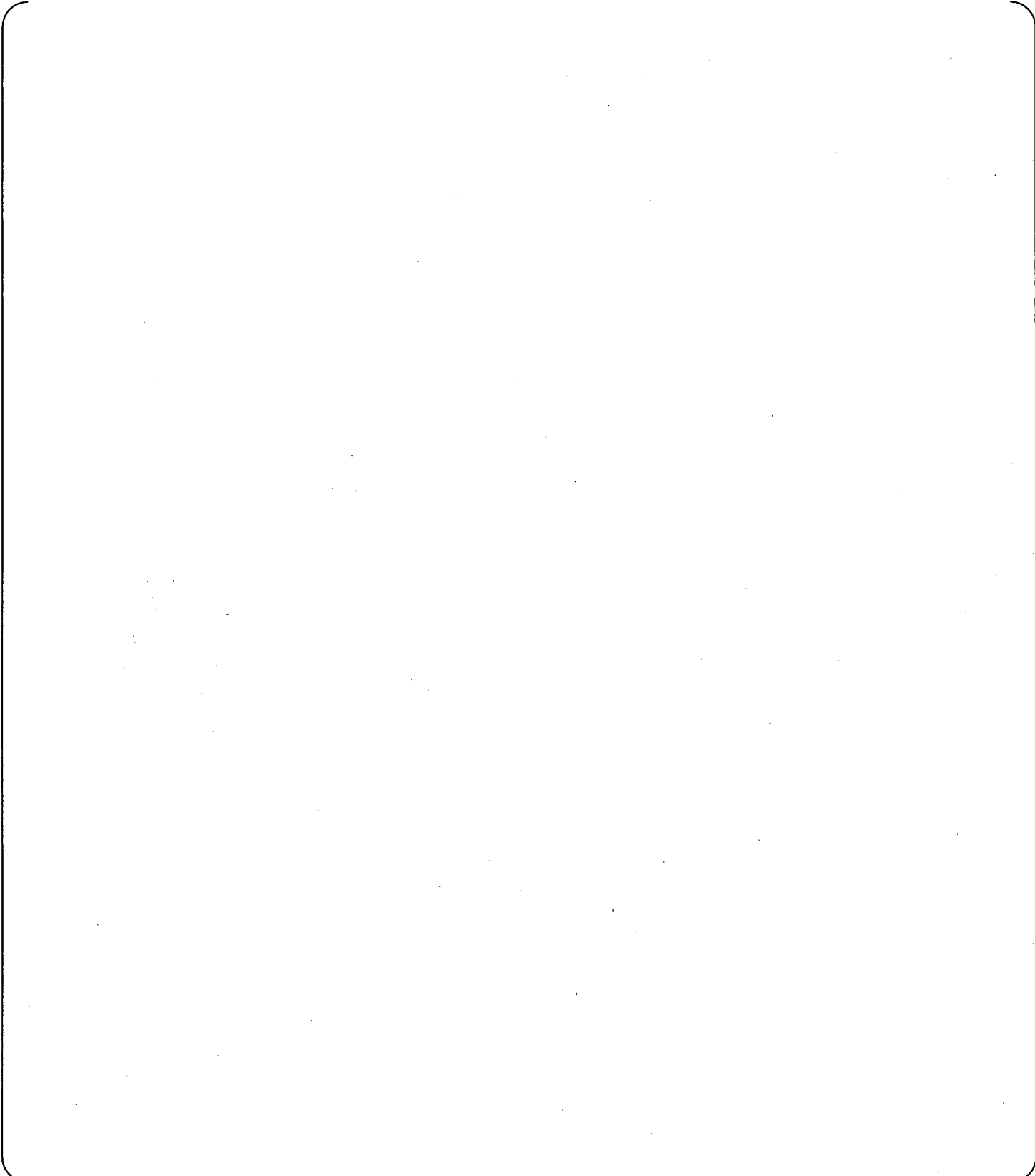
Fig. 11-1 Outline Drawing of the Flow Damper

RAI 12.

During the low flow injection regime, is there a flow from the standpipe and what is the ratio between the two flows, from the standpipe and from the side pipe? If the standpipe flow is zero, the device is like a vortex diode instead of a vortex triode. In the case of a diode, the resistance is a function of the ratio of radii of outer wall and of the inlet of the injection pipe for the inviscid flow. Is this also applicable for a triode?

Response

Yes, the resistance is a function of the ratio of radii of outer wall and of the throat of the outlet nozzle for the inviscid flow. The flow velocity from the large flow pipe is 1/169 that from the small flow pipe and is negligible during small flow rate oeration. The invicid flow theory can also be useful to predict the performance of the flow damper, but there are velocity boundary layers on the upper and lower disks that make flow in the vortex chamber complex. That complexity is the reason for the flow rate characteristics to deviate from what inviscid flow theory would predict making it necessary to assess flow damper performance through experiments.

<u>RAI 13.</u>

What is the effect of wall friction from different walls in the vortex chamber?

<u>Response</u>

The wall friction makes the flow in the vortex chamber complex. A pair of velocity boundary layers develops on the upper and lower disk walls of the chamber. Centrifugal force in these layers is weak, and pressure drop across the radius of the chamber induces a higher flow velocity in those largers than in the midplane of the chamber.

RAI 14.

There are three flow regimes in the vortex chamber: near the outer wall, middle section, and near the entrance to injection pipe. It is shown (Kirshner and Katz book, Academic Press, 1975, Pages 280-283) that there is a recirculation in the middle region between two horizontal surfaces where most of the losses will occur. How is the scaling done for the vortex chamber so that the loss coefficient is the same for the ½ scale and full scale facility. Also, what is the effect of the height (vertical dimension) of this chamber on the flow?

Response

The boundary layers on the upper and lower disk walls make the flow in the vortex chamber complex. The flow-rate coefficient depends on the ratio of the height to the diameter of the vortex chamber. MHI did not observe reverse flow in the vortex chamber of the 1/5-scaled model in the flow visualization tests. We infer that the recirculation region stated in the book mentioned above was measured with relatively small diodes at a low Reynolds number because fluidic components were generally tested and investigated with small models. The effect of viscosity on flow diminishes as the Reynolds number becomes large. that is the reason why MHI used a relatively large model with scale of 1/5 or larger, in other words 360mm in diameter or large, in order to gather data in the large Reynolds regime. In addition, the data of the 1/2-scale model were compared with those of the 1/5-scale model to assess the effect of viscosity. This comparison showed there was a almost no digression of the data of the 1/5-scaled model from those of the 1/2-scaled model, even though the ratio of the Reynolds numbers of these models was about 1/10, as mentioned in Chapter 4.3 of the Topical Report. Since the ratio of the Reynolds numbers of the 1/2-scale model and the actual flow damper is only 1/2, the digression of the data of the actual flow damper from those of the 1/2-scale model must be much smaller than these.
The interpretation of this phenomenon is as follows:
The growth of the boundary layers on the disk walls will be suppressed by large Reynolds numbers and acceleration along the radius of the vortex chamber. The pressure drop will be generated by the acceleration in the vortex chamber, and most of the energy loss will occur in the region between the exit of the chamber and the diffuser downstream the orifice due to the shear stress at the center of the vortex and on the wall. Hence the amount of the energy loss is determined by the flow in the vortex chamber, even though the loss occurs thereafter. If the boundary layers in the vortex chamber change little because of high Reynolds numbers, the amount of the energy loss will be same regardless of model size.

RAI 15.

Equation 4.2 in the topical report defines Froude number. What is typical velocity? Why is the standpipe diameter a right length scale?

Response

The typical velocity (characteristic velocity) is 1.2 to 1.6 m/s in the standpipe of the model at flow switching, as shown in Table 4.2.2-1 in the Topical Report.
The Froude number is an indication of the gravity effect on the behavior of the water surface in the accumulator tank. Therefore, the height of the standpipe was chosen as the characteristic length of the Froude number for the 1/5- and 1/2-scale models in order to investigate the transient of the water level in the standpipe.
The 1/3.5-scale model should have used the height of water over the standpipe as the characteristic length of the Froude number in order to investigate the behavior of the water surface in the tank. However, the height of water varies with time and is not a suitable representation of the characteristic length. Since the diameter of the test tank and the configuration of the portion of the inlet of the standpipe were similar to those of the actual ones, any portion similar to that of the prototype can be chosen as the characteristic length. MHI chose the diameter of the standpipe in place of the varying height of water to ensure the applicability of the test data to the actual accumulator. For reference, the ratio of the height to the equivalent diameter of the standpipe is 5.57(=3253/584.3).

RAI 16.

Tables 4.2.3-1 and 4.2.3-2 summarize the conditions for different tests for the 1/5 scale facility. What is the difference between Tests 1/5-1-1 and 1/5-2-1?

Response

The test conditions are the same between Tests 1/5-1-1 and 1/5-2-1. No. 1/5-1-1 is the run number of the visualization test and No. 1/5-2-1 is the run number of the test from which the flow characteristics were obtained.

RAI 17.

The figures for the 1/5 scale facility (Section 4.2.3) have data for different tank pressures. However, there is no trend of pressure dependencies on cavitation factor. Why?

Response

Here is the summary of the ranges of cavitation factors in each test.

Test No.	Initial Tank Pressure	Cavitation Factor at Large Flow	Cavitation Factor at Small Flow
1/5-2-1	128 psig	4 ~ 5	0.4 ~ 0.6
1/5-2-3	42 psig	3 ~ 7	2 ~ 3
1/5-2-2	29 psig	1 ~ 5	4 ~ 10

For large flow, the higher initial tank pressure shows a larger cavitation factor. On the other hand, for small flow, the trend appears to be the reverse.

Because the effect of vapor pressure is very small, the cavitation factor is similar to the ratio of absolute pressure at the outlet of flow damper to the pressure loss of the flow damper. If the initial tank pressure is higher, the flow rate becomes larger, and the pressure loss of flow damper also becomes larger. Since the pressure of the backpressure tank is constant (atmospheric pressure), a large flow rate causes a large pressure drop at the injection pipe, and the pressure at outlet of flow damper becomes higher.
It shows that if the initial tank pressure is higher, both the numerator and the denominator of the definition equation of cavitation factor become larger.
In other words, the initial tank pressure does not unilaterally make cavitation factor large or small.

RAI 18.

For the ½ scale facility (Figures 4.2.4), what controls the standpipe water level? It varies from case to case right after the switch from large flow to small flow.

Response

The water level transient in the standpipe during switchover the injection flow rate of advanced accumulator is represented in the following Equation (18-1).

$$\frac{d}{dt}(lV) = \underbrace{-\frac{Q_1}{A}V_2}_{(a)} + \underbrace{g(l_v - h)}_{(b)} - \underbrace{(\zeta + Cd)\frac{1}{2}|V|V}_{(c)} - \underbrace{(1 - Cp)\frac{1}{2}V_1^2}_{(d)} \qquad (18\text{-}1)$$

h	:Tank water level (m)
l	:Water column length (m)
l_v	:Water column height (m)
V	:Velocity in standpipe (m/s)
V_1	:Velocity in small flow pipe (m/s)
V_2	:Velocity in large flow pipe (m/s)
Q_1	:Flow rate in standpipe (m³/s)
A	:Inner area in standpipe (m²)
g	:Acceleration of gravity (m/s²)
ζ	:Standpipe elbow resistance (-)
Cd	:Standpipe resistance (-)
Cp	:Friction loss of small flow pipe (-)
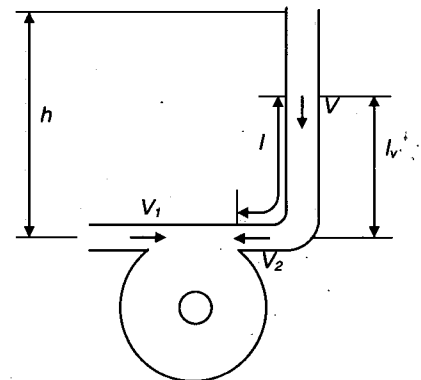
Calculation model for standpipe water level transient

Equation (18-1) is the dynamic equation per unit area regarding factors for momentum change of water column, and each term represents following:

Left-hand side: Momentum change of water column
Right-hand side:
             (a)…Momentum change by outward flow
             (b)…Force to water column by differential water head
             (c)…Force of pipe resistance
             (d)…Force at outlet of water column

Maximum decrease of the standpipe water level based on a calculation model as Equation (18-1) is shown in Figure 18-1. The estimated water level reduction shows good agreement with the test results (measured data).

The reason why the standpipe water level varies from case to case right after the switch from large flow to small flow is that the velocity in the standpipe varies right before the switch of flow rate. In case 3, which has the highest initial tank pressure, the velocity in standpipe before the switch of flow rate is the highest and the decrease of water level is the largest.
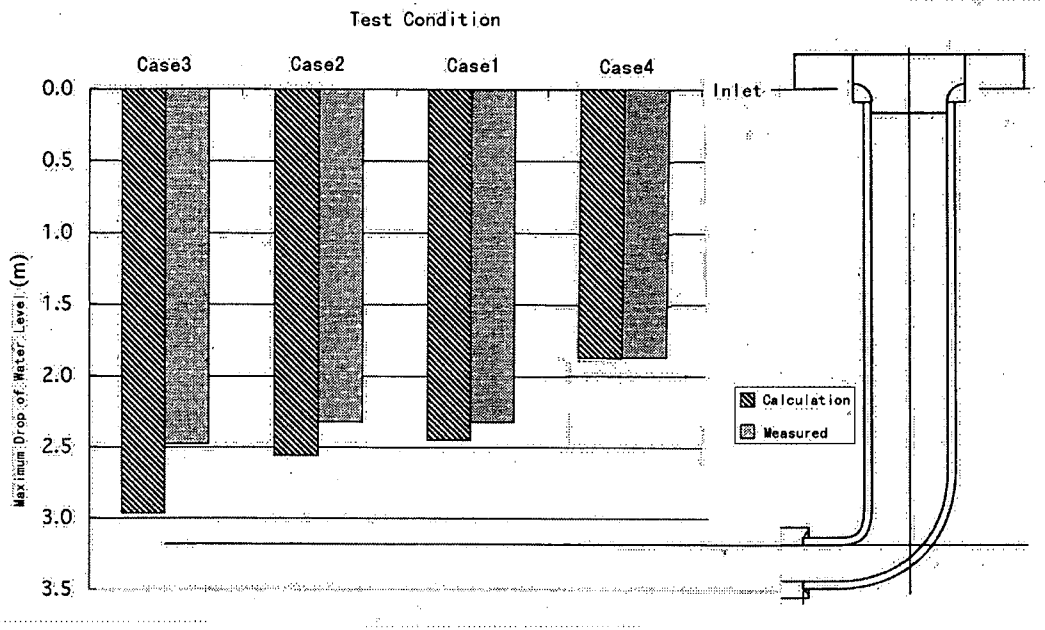
Fig.18-1 Max. Decrease in the Standpipe water level

RAI 19.

For the ½ scale facility (Figures 4.2.4), the peak flow rates vary in magnitude and timing from case to case. Why?

Response

The peak flow rates were observed while the outlet valves were fully opened (approximately 3.5 seconds) in every case. The variations of the magnitude of the peak flow rates depend on the differences between the initial test tank pressure and the exhaust tank pressure. Basically, if the difference between these pressures is larger, the peak flow rate also becomes larger.
In case 1 and case 4, the initial pressure of the test tanks were the same, but the pressures of the exhaust tank were different (case 1: 14 psig, case 4: 71 psig).
In case 4, despite having a differential pressure was smaller than that for case 1, the peak flow rate was larger than in case 1. This was because the backpressure was higher in case 4, so that the cavitation factor became larger, and the flow coefficient also became larger, than those for case 1.

RAI 20.

For the ½ scale facility (Figure 4.2.4-11), why does Case 1 have lower cavitation factors than Case 7 when Case 1 is for higher pressure?

Response

The magnitude of the cavitation factors does not depend on the test tank pressure solely. The cavitaion factor is defined by Equation (4-9) of the Topical Report. Because the effect of the vapor pressure is very small, the cavitation factor is similarly the ratio of the absolute pressure at the outlet of flow damper to the pressure loss of flow damper. To obtain a larger cavitation factor, the flow damper outlet pressure would need to be larger and the pressure loss in the flow damper would need to be smaller. In case 1, both the flow damper outlet pressure and the pressure loss are larger than those for case 7, so the higher pressure does not translate into a larger cavitation factors.

RAI 21.

In the response to NRC question 13-B, the threshold cavitation factor, s_{th}, below which cavitation can occur, is derived based on the one dimensional momentum equation (the fourth equation).

Please show how the one dimension momentum equation is obtained and used.

Response

At first, a control volume is defined as shown in Figure 21-1. The one-dimensional equation of momentum conservation along the axis of the diffuser pipe is written as:

$$\left[\qquad\qquad\qquad\qquad\qquad \right] \qquad (21\text{-}1)$$

where the 1st term on the left hand side represents the force acting on the bottom of the control volume, the 2nd term the force on the wall of the diffuser, the 3rd tem the momentum coming in the bottom of the control volume, the 1st term on the right hand side the force acting on the top of the control volume and the 2nd term the momentum going out the top of the control volume. For simplicity, assuming $P_w = P_t$, then Equation (21-1) reduces to

$$\left[\qquad\qquad\qquad\qquad\qquad \right] \qquad (21\text{-}2)$$

The notation of the diameter of the injection pipe is $d_2 = d_p$ in the equation that was shown in the Response for Question 13-B in the first set of RAIs. Since the equation of continuity is

$$\left[\qquad\qquad\qquad\qquad\qquad \right] \qquad (21\text{-}3)$$

Equation (21-2) can be rewritten as:

$$\left[\qquad\qquad\qquad\qquad\qquad \right] \qquad (21\text{-}4)$$

Hence, the cavitation factor can be expressed as:

$$\left[\qquad\qquad\qquad\qquad\qquad \right] \qquad (21\text{-}5)$$

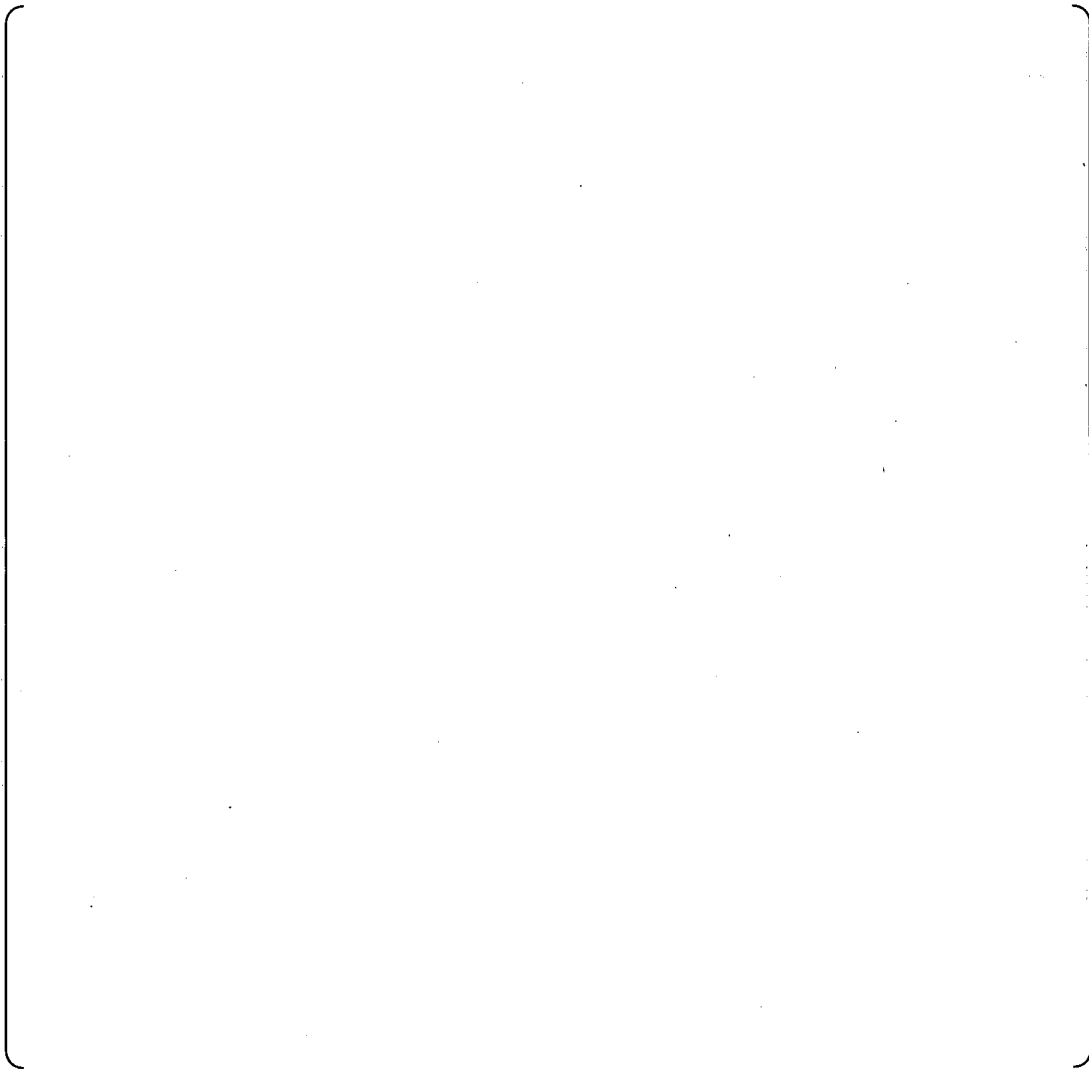which is the third equation of the Response to Question 13-B.

Fig. 21-1 Control Volume

Note: A more rigorous discussion is possible, as follows:
Define the pressure coefficient on the wall of the diffuser, C_p, as

$$\left[\right] \tag{21-6}$$

The mean pressure coefficient on the wall of the diffuser is defined as

$$\left[\right] \tag{21-7}$$

Then, Equation (21-1) can be written as

$$\left[\right] \tag{21-8}$$

Hence, the cavitation factor is written as

$$\left[\right] \quad \text{(21-9)}$$

The threshold, σ_{th} at which cavitation can occur, is

$$\left[\right] \quad \text{(21-10)}$$

To estimate this value, the mean pressure coefficient, $\overline{C}_p$, must be given. If $\overline{C}_p = 0$, Equation (21-10) reduces to the threshold equation mentioned in the Response to Question 13-B.

RAI 22.

The response to NRC question 17-A is not clear. Please provide the numerical values of the time periods suggested in this question, such as early, middle and late injection during large flow period.

Response

The time periods for error evaluation of flow coefficients are shown in Table 22-1. The short periods are set up as the time zone at error evaluation. The mean values of the flow coefficients in each short period were described in Table 17-2 in the answer to NRC question 17-A.

Table 22-1 Time zone at error evaluation in test case 1

Teat case	Time zone at error evaluation (sec)					
	Large flow rate			Small flow rate		
	Early	Middle	Late	Early	Middle	Late
1						
2						
3						
4						
5						
6						
7						

MHI's Responses to NRC's RAI on   )onses to NRC';
Advanced Accumulator for US-APWI Accumulator fo
Topical Report MUAP-07001-P (R1)   port MUAP-070(

RAI 23.

In the response to NRC question17,onse to NRC q
17.2? Eq. 4.7 in main report does n4.7 in main rep

Response   !

In the topical report (page 4.2.3-4, sal report (page
flow damper outlet piping) and V_D (\er outlet piping'

Note: These parameters were the ese parameter:

To convert the measured static pres the measured
velocity in the flow damper outlet pijthe flow dampe
of test facilities are used.   lities are used.
Since commercial piping is used in 1mercial piping i
strictly scaled relative to the actual pled relative to t

The pressure loss of the flow dampure loss of the 1
outlet. Since the total pressure of thce the total pre
parameters are converted by the fols are convertec

$$P_D + \rho \cdot V_D^2 / 2 = P_D' + \rho \cdot V_D'^2 \text{ /o} \cdot V_D^2 / 2 = P_D'$$

$$P_D = P_D' + \rho \cdot V_D'^2 / 2 - \rho \cdot V_D^2 / P_D' + \rho \cdot V_D'^2 / \text{'}$$

$$V_D = V_D' \cdot (D'/D)^2 \qquad \qquad \text{'}_D' \cdot (D'/D)^2$$

Where
P_D : Static pressure of flow dampatic pressure o'
P_D' : Static pressure of flow dampatic pressure o'
V_D : Velocity of the actual scale ılocity of the ac
V_D' : Velocity of the test facility pılocity of the te:
D   : Diameter of the actual scaleameter of the a
D'   : Diameter of the test facility ameter of the t(
ρ : Density of water   ınsity of water

RAI 23.

In the response to NRC question17-B, why are there two separate diameters in Eq. 17.2? Eq. 4.7 in main report does not show this.

Response

In the topical report (page 4.2.3-4, section 4.2.3, 3 (b) (2)), the notes of P_D (Static pressure of flow damper outlet piping) and V_D (Velocity in the flow damper outlet piping) states as follows:

Note: These parameters were the values converted to the scale of the actual ACC.

To convert the measured static pressure of flow damper outlet piping P_D', and measured velocity in the flow damper outlet piping V_D' to the actual P_D and V_D, inner diameters of piping of test facilities are used.
Since commercial piping is used in the test facilities, the inner diameter of the piping cannot be strictly scaled relative to the actual piping. For that reason, these conversions are performed.

The pressure loss of the flow damper is the total pressure differential between the inlet and the outlet. Since the total pressure of the actual piping is the same as that of the test facilities, parameters are converted by the following equations:

$$P_D + \rho \cdot V_D^2 / 2 = P_D' + \rho \cdot V_D'^2 / 2$$
$$P_D = P_D' + \rho \cdot V_D'^2 / 2 - \rho \cdot V_D^2 / 2$$
$$V_D = V_D' \cdot (D'/D)^2$$

Where
P_D : Static pressure of flow damper outlet piping for the actual scale piping
P_D' : Static pressure of flow damper outlet piping for test facility
V_D : Velocity of the actual scale piping
V_D' : Velocity of the test facility piping
D   : Diameter of the actual scale piping
D'   : Diameter of the test facility piping
ρ : Density of water

RAI 24.

In the response to NRC question 17, what do the relative influence coefficient and degree of freedom mean in Tables 17-1 and 17-2?

Response

ANSI/ASME PTC19.1-1985, "Performance Test Code Part 1, Measurement Uncertainty, Instrument and Apparatus," Section 4.2, "Calculation Procedure" provided the following description for reporting the result of uncertainty analysis: "The report summary should contain the nominal level of the test result, bias limit, precision index, degree of freedom, and the uncertainty of the test result, stating the model used." In accordance with this description, the calculated results of the uncertainty of flow rate and flow coefficient, bias limit and precision index of each individual parameter used in the uncertainty calculation, and their influence coefficient and degree of freedom used to calculation, are listed in Tables 17-1 and 17-2 in "Response to NRC's Questions"

The relative influence coefficient is used to propagate each parameter's errors into a result. In Table 17-1 in "Response to NRC's Questions", relative bias limit and relative precision index of flow rate of parameter 4, which are the end products, are calculated by using relative influence coefficients of individual parameters 1, 2, and 3. The calculation expression is described in page 34 of "Response to NRC's Questions".
Similarly, in Table 17-2 in "Response to NRC's Questions", the relative bias limit and relative precision index of flow rate coefficient of parameter 7, which are the end products, are calculated by using the relative influence coefficients of individual parameters 1, 2, 3, 4, 5, and 6. The calculation expression is described in page 35 of "Response to NRC's Questions".

The degree of freedom is used in calculating uncertainty of 95% coverage, summing up relative bias limit and precision index of flow rate and flow rate coefficient. The calculation expression is described in page 36 of "Response to NRC's Questions." The degree of freedom in the tables also shows that samples of "degree of freedom $v +1$" are used in calculating relative bias limit of each parameter.

RAI 25.

The response to NRC question 18 is related to the manufacturing errors. However, in all estimates of corresponding biases in the flow coefficient, it is assumed that the velocity is not affected. Is there an effect of the manufacturing errors on loss coefficients? For large flow conditions, the facing angle error contribution to the bias is 1.2%. How is this estimated? Any off design condition (such as facing angle error) will lead to vortex formation and increase in losses. Please explain.

Response

During the large flow injection, there is no vortex in the vortex chamber or the throat. The flow rate is controlled by the throat that has the minimum cross sectional area along the flow path. The manufacturing error of the throat may slightly change the cross sectional area but has negligible effect on the velocity in the throat. The reason is as follows: The accelerated flow in the reducer upstream the throat has negligible friction loss. The decelerated flow in the diffuser downstream the throat has no flow separation because of its small zenith angle, so the effect of the manufacturing error of the throat on the friction loss of the diffuser is too small to assess. Consequently, the manufacturing error of the throat on the flow velocity is negligible. During the small flow injection, the centrifugal force controlling the flow rate coefficient, or flow resistance coefficient, is a function of the ratio of the diameters of the vortex chamber and the throat that was assessed in Response to Question-18 of the first set of RAIs.

RAI 26.

Section 4.2.4 of the topical report, regarding the full-height ½ scale tests, states that
pressure, water level, and temperature were measured by the instruments shown in
Figure 4.2.4-1 for all test cases and used to calculate the cavitation factor and the flow
rate coefficient.

a. How is the flow rate in the injection pipe in the scaled tests measured or calculated,
   and where is that data shown in the topical report (In Figures 4.2.4..)?

b. Once a flow establishes due to a difference in pressure between the ACC tank and
   the external system pressure, what happens to the mass flow rate versus time
   curves shown in Section 4.2.4 figures when the external system pressure varies
   during the transient (this could be due to various feedbacks from the break)?

Response

a.
The flow rate is obtained by the following equation using the test tank water level data shown
in Attachment 1.

$$Qn = \left(L_{n-1} - L_{n+1}\right) \cdot \left(\pi \cdot Dt^2 / 4\right) / \left(T_{n+1} - T_{n-1}\right)$$

Qn	: Flow rate at time T_n (m³/s)
T_{n+1}	: Time of n+1th Data
T_{n-1}	: Time of n-1th Data
L_{n-1}	: Test tank water level at time T_{n-1} (m)
L_{n+1}	: Test tank water level at time T_{n+1} (m)
Dt	: Test tank inner diameter (m)

b.
As discussed in the topical report section 5.1, injection flow rate according to the variation of
external system pressure can be calculated by an analysis code that incorporates equations 5-
1 and 5-2 of the topical report. Accumulator injection flow transients during the LOCA with
different break sizes are shown in Figure 15-6-5-7, 17, 26, DCD Section 15 of US-APWR.

RAI 27.

The level of water in the accumulator tank is used to quantify the exit mass flow rate but, as our preliminary CFD shows, the level of the water is not uniform across the tank.

How is this discrepancy accounted for during level calculations?

Response

The water level in the test tank was measured by a differential pressure transducer. Hence, the variation of water level across the tank does not affect the evaluation of the flow rate injected.
Since the water in the tank is quiescent at the beginning of injection, there is no cause to disturb the water surface during large flow rate injections. This quiescent state of the water surface was observed by the 1/3.5-scale model. At a flow rate change, the water surface may be disturbed due to the exposure of the anti-vortex cap out of the water, but the disturbance is limited during the short time of flow-rate switching. During small flow rate injections, the waves in the water surface generated by the disturbance of the flow-rate switching will diminish soon and subsides untile the water is quiescent.

RAI 28.

The NRC staff is conducting an in-depth study of the advanced accumulator (ACC) using computational fluid dynamics (CFD) calculations. Please provide detailed dimensional drawings of the1/2 scale test ACC model and the actual full scale ACC, and in particular. The dimensions of the anti-vortex caps and their connections to the standpipe and small flow pipe.

Response

Detailed dimensional drawings of the full height 1/2 scale test ACC model are shown in Figure 28-1 through 28-4.

MHI has not yet prepared similar drawings of actual scale as those for the 1/2 scale. All flow path dimensions for the full scale flow damper will be double those of the full height 1/2 scale test, except for the standpipe height (refer to Table 11-1).

Figure 28-1

Vortex Chamber (Full height 1/2 scale model)

Figure 28-2
Flow Nozzle (Full height 1/2 scale model)

| Figure 28-3 |
| Stand Pipe (Full height 1/2 scale model) |

Figure 28-4
Schematic of Facility (Full height 1/2 scale model)

RAI 29.

Explain under what conditions and at what liquid level in the accumulator, there will be entrainment of nitrogen from the gas space, and injection to the reactor vessel? What will the flow rate for this nitrogen be? Are there any data on this type of nitrogen injection?

Response

During small flow injection, a water level difference between the standpipe and the tank is developed as shown in Figure 29-1.

The following equations hold for each small and large flow pipe, based on Bernoulli's theory:

$$P_g = P_0 + \frac{1}{2}\rho V_1^2 - \rho g H_1 \qquad (29\text{-}1)$$

$$P_g = P_0 + \frac{1}{2}\rho V_2^2 - \rho g H_2 \qquad (29\text{-}2)$$

Equation (29-1) and (29-2) yield:

$$\frac{1}{2}\rho V_1^2 - \rho g H_1 = \frac{1}{2}\rho V_2^2 - \rho g H_2 \qquad (29\text{-}3)$$

Where,

P_0	:	Static pressure at confluence area
P_g	:	Tank gas pressure
ρ	:	Density of water
V_1	:	Velocity at small flow inlet
V_2	:	Velocity at large flow inlet
H_1	:	Tank water level
H_2	:	Standpipe water level
g	:	Gravity acceleration

In turn, equation (29-3) yields:

$$\frac{1}{2}\rho V_1^2 - \frac{1}{2}\rho V_2^2 = \rho g(H_1 - H_2) = \rho g \Delta H \qquad (29\text{-}4)$$

Where,

ΔH : Water level difference between the standpipe and the tank

---

Thus, the water head difference is developed as the difference of dynamic pressure between the small flow inlet and the large flow inlet.

During small flow injection, since the velocity at the small flow inlet (V_1) is greater than the velocity at the large flow inlet (V_2), the water level in the standpipe becomes lower than that in the tank (i.e., $H_2 < H_1$).

As described above, the water level in the standpipe becomes lower than the water level in the tank due to the dynamic pressure difference between small flow inlet and large flow inlet, and the standpipe water level reaches top of vortex chamber faster than the tank water level. However, the full height 1/2 scale test confirmed that the stable flow rate transition is obtained for a period after the standpipe water level reaches the top of vortex chamber.

Figure 29-2 and Figure 29-3 show the water level transient and flow rate transient, respectively, in the full-height, 1/2 scale test case 1 (initial tank pressure is 586 psig) , and Figure 29-4 and Figure 29-5 show the water level transient and flow rate transient, respectively, in the full-height 1/2 scale test case 3 (initial tank pressure is 758 psig [Note 1]).

In case 3, the standpipe water level reaches the top of vortex chamber before the test termination, but tank water level and flow rate transition are still smooth as in test case 1, and flow characteristics of flow damper are not affected by the standpipe water flow during the test period. [Note 2] Even though the standpipe water level reaches the top of vortex chamber, flow from the small flow pipe plugs the large flow inlet and nitrogen gas entrainment from standpipe does not occur immediately.

Nitrogen gas entrainment would occur at the period that the flow from the small flow inlet decreases and could not plug the large flow inlet as the progress of injection.

However, as described in note 2, MHI has no data regarding nitrogen injection since all parameters were measured until the time that the test tank water level reached 3.77 ft above the vortex chamber in the full-height 1/2 scale test.

Note 1: Initial condition of high pressure which does not exist in the actual accumulator.

Note 2: In the test, all parameters were measured until the time that tank water level reached the level (3.77 ft above the top of vortex chamber) correspond to the injection water volume expected in safety analyses.
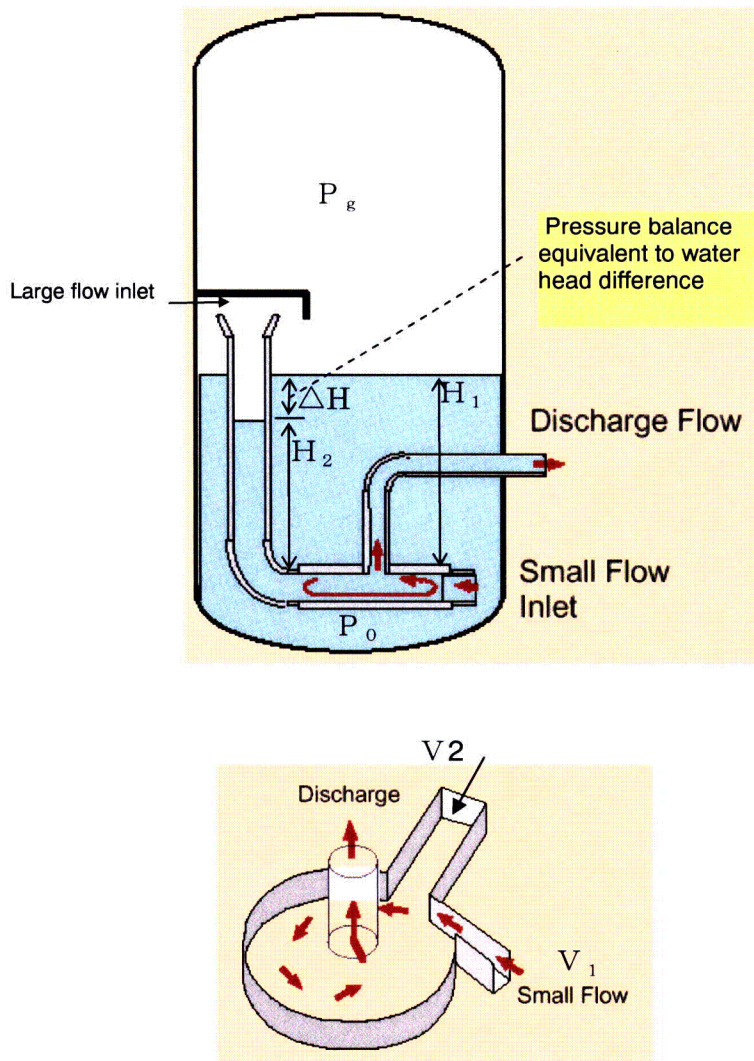
Figure 29-1 Water level in tank and standpipe during small flow injection
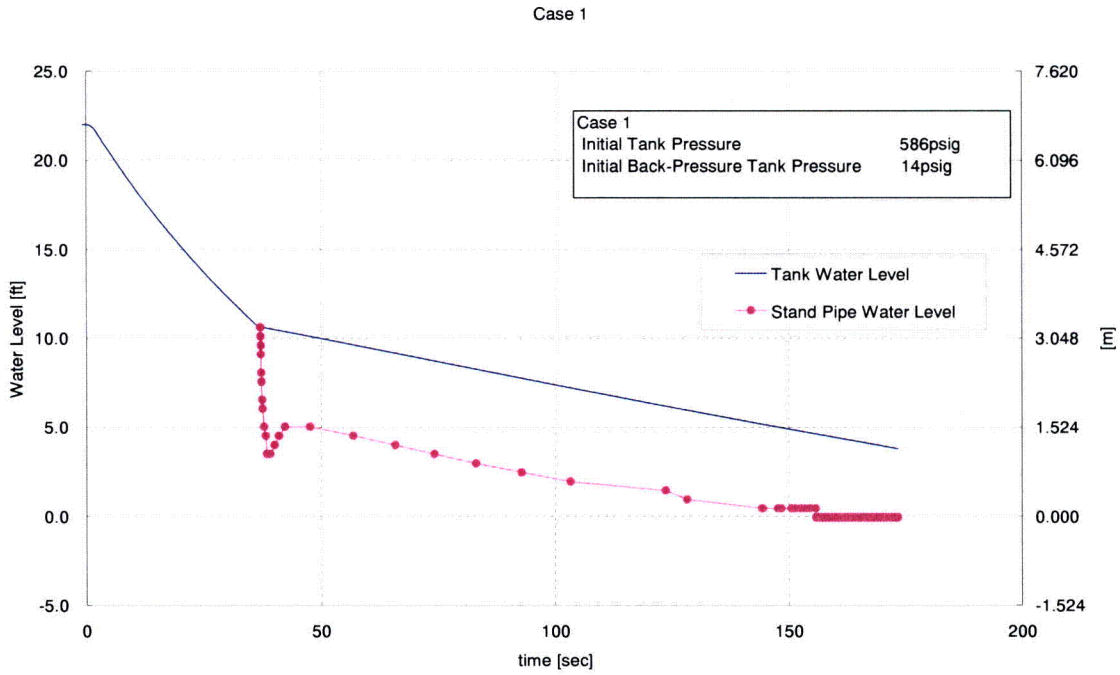
Case 1

Figure 29-2 Water level transient in full-height 1/2 scale test case 1
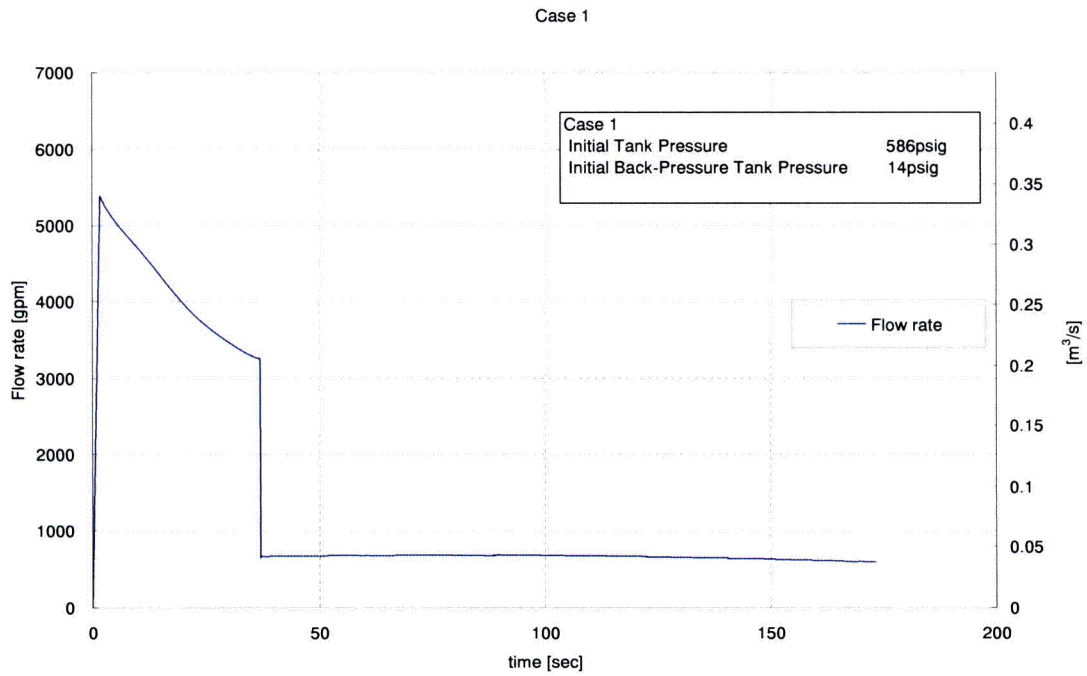
Case 1

Figure 29-3   Injection flow rate transient in full-height 1/2 scale test case 1
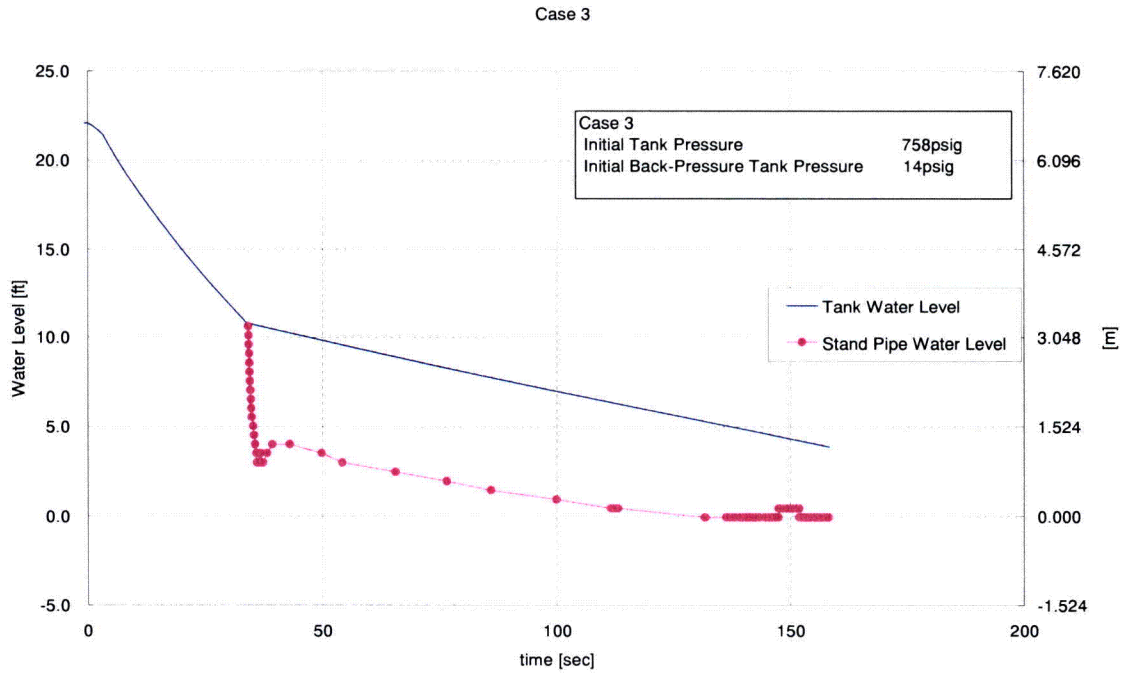
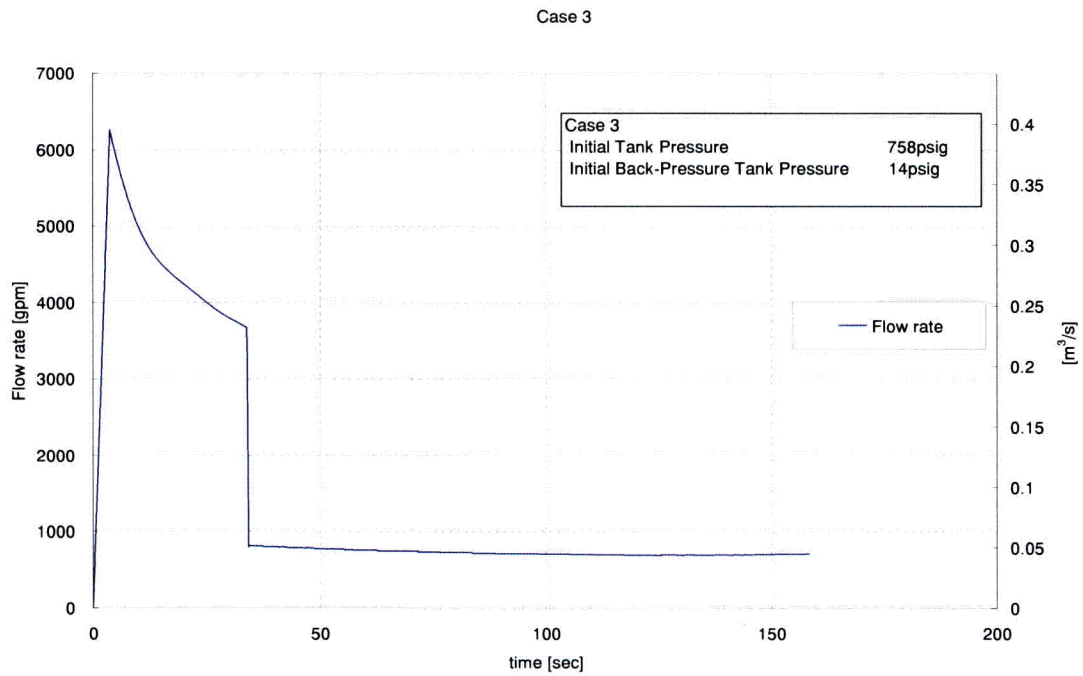Figure 29-4 Water level transient in full-height 1/2 scale test case 3

Figure 29-5 Injection flow rate transient in full-height 1/2 scale test case 3

Figure 1 In reference to RAI questions 2, and 27
Our preliminary model consist of a cylindrical accumulator tank housing features seen in the
Advanced Accumulator such as the large flow pipe, small flow pipe, vortex chamber, throat,
and
injection pipe. Fluent 6.3.26 was used for the analysis and due to the multiphase flow nature of
the problem the Mixture Model and Cavitation Model were involved. The initial tank pressure
was set at 4.04 MPa (gage), pressure at the injection outlet pipe decreases linearly from the
initial tank pressure to 0.098 MPa (gage).

Side 1   (2-D)   Side 2   (3-D)